An Improved Method for Virtual Air Gap Length Computation

Adalbert Konrad[1], *Fellow, IEEE,* and Jean F. Brudny[2], *Senior Member, IEEE*

[1]Department of Electrical and Computer Engineering, University of Toronto, Toronto, ON, Canada M5S 3G4
[2]Director, LSEE Electrical Engineering Department, University of Artois, Technoparc Futura, 62400 Bethune, France

This paper presents an analytical approach to the analysis of a single-phase transformer with a virtual air gap. Four auxiliary windings with dc currents that locally saturate the core are embedded in the transformer core. Due to changes in the magnetic characteristics of the core a virtual air gap is created. The method focuses on the change in transformer core reluctance with local saturation and on obtaining the equivalent mechanical length of the virtual air gap. The accurate calculation of the magnetic field in the core is necessary to obtain both the operating point of the core and the change in core reluctance. Results obtained from the proposed method are compared with experimental and analysis results available in the literature.

***Index Terms*—Air gap, method of images, transformers.**

I. Introduction

AN APPROACH to the analysis of a single-phase transformer with a virtual air gap is presented. The transformer geometry and physical dimensions are shown in Figs. 1 and 2, respectively. The measured magnetization curve of the core material is given in Fig. 3. The transformer has four auxiliary windings embedded in its core and connected to a dc supply. The purpose of these windings is to locally saturate the core. By changing the core permeability in the region of the auxiliary windings, a virtual air gap is created, which combined with electronic circuitry, has potential application in resonant converters, elimination of harmonics, and transformer inrush current reduction [1].

An equivalent mechanical air gap length, of interest to designers, can be associated with the virtual air gap. It results from an increase in core reluctance with local saturation and is obtained by an analytical approach based on finding the distribution of the magnetic field in the core produced by the auxiliary windings. The accurate calculation of the magnetic field is necessary to obtain both the operating point of the core and the change in core reluctance.

The proposed method consists of five steps. Steps 1, 2, and 5 are identical to aspects of the approach described in [2]. However, steps 3 and 4 are new [3]. The result obtained from the proposed method is compared with experimental and analytical results presented in [2].

II. Description and Application of the Method

The five steps of the proposed method are described under separate headings below.

A. Core Reluctance Without Local Saturation

Step 1 is to obtain the reluctance of the core with uniform cross section *without* local saturation. The ac voltage applied to the main windings produces a peak magnetic flux $\Phi_{\rm m}$. The corresponding current is obtained from the magnetization curve and the mmf required without local saturation is found. Denoting the mmf by $\Im_{\rm m}$, the reluctance becomes

$$\Re_{\rm m} = \frac{\Im_{\rm m}}{\Phi_{\rm m}} = \frac{23.93}{5.359 \times 10^{-4}} \text{A-t}/Wb = 44653.85 H^{-1}. \quad (1)$$

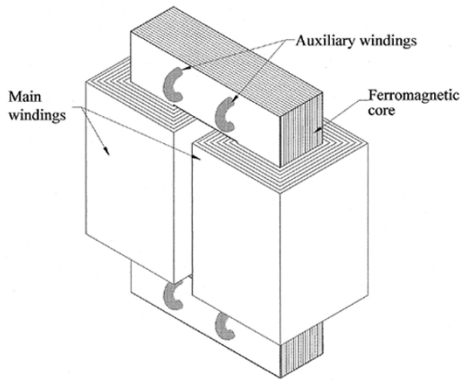

Fig. 1. Transformer geometry showing 3-D windings and core.

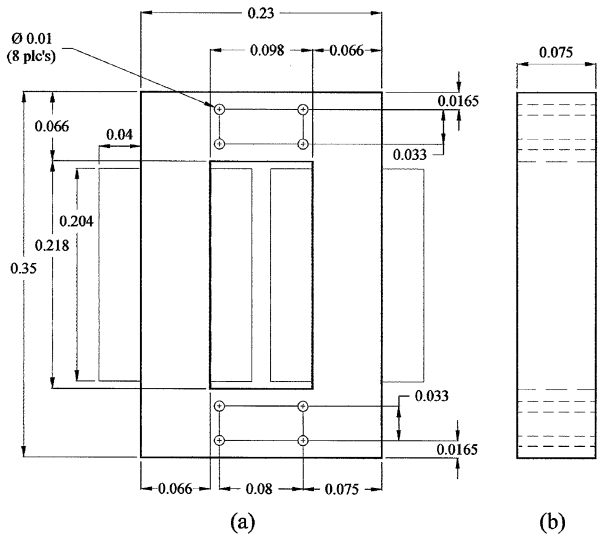

Fig. 2. Transformer core and winding dimensions in meters.

Digital Object Identifier 10.1109/TMAG.2005.854987

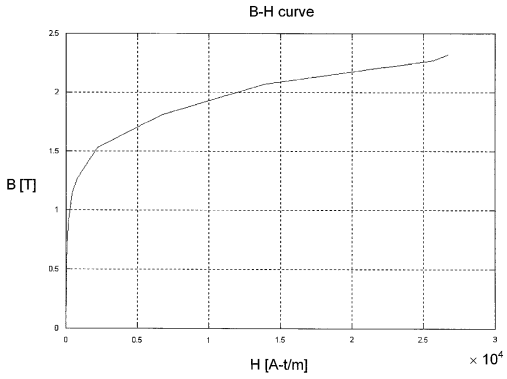

Fig. 3. Measured magnetization curve of the core material.

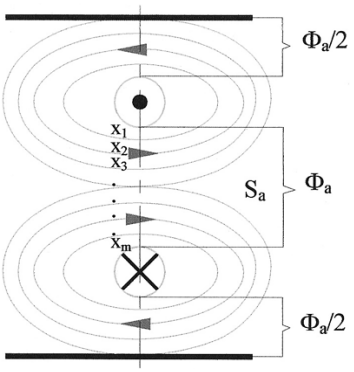

Fig. 4. Tubes x_1 through $x_{\rm m}$ around an auxiliary winding.

B. Computation of Auxiliary Magnetic Field

Step 2 is the calculation of the auxiliary magnetic field H_a when a dc current of $I_a = \pm 10$ A is applied to the auxiliary windings. The region of core across the center of the auxiliary windings is divided into m tubes of different lengths (Fig. 4). An average value of H_a is obtained by the image method described in [2]. H_a is then used to obtain the flux Φ_a around the auxiliary windings. The windings come in pairs, so the direction of dc magnetic flux around the conductors has no bearing on performance.

C. Induction in the Auxiliary Windings

Step 3 is to take into account the induction in the auxiliary windings. $\Phi_{\rm m}$ induces a voltage and an ac current appears in the auxiliary windings. Assuming simple transformer action between main and auxiliary windings, the latter produces a peak magnetic flux Φ'_a of its own with a magnitude equal to $-\Phi_{\rm m}$. The dc currents produce flux Φ_a whose value depends on H_a. The total flux, Φ_{ta}, of the auxiliary windings, is given by

$$\Phi_{ta} = \Phi_a + \Phi'_a = \Phi_a - \Phi_{\rm m}. \tag{2}$$

Clearly, Φ_{ta} is smaller than Φ_a. The reduction is equivalent to a decrease in the current applied to the auxiliary windings. Therefore, the total auxiliary magnetic field, H_{ta}, is smaller than H_a. Fig. 5 compares the distributions of H_a and H_{ta} in one quarter of the core.

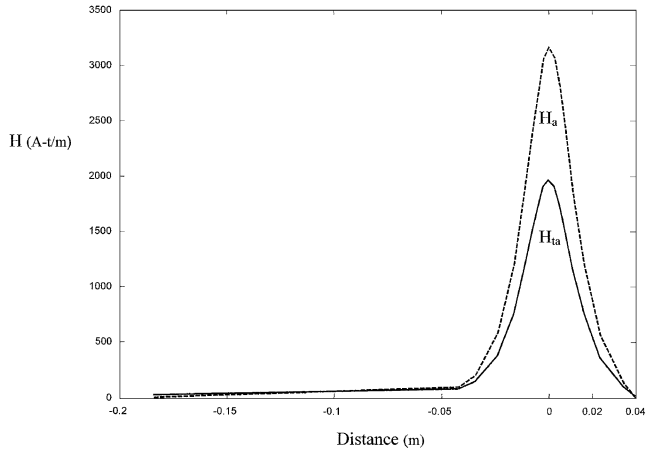

Fig. 5. 1D fields H_a and H_{ta} along mean length of $1/4$ core.

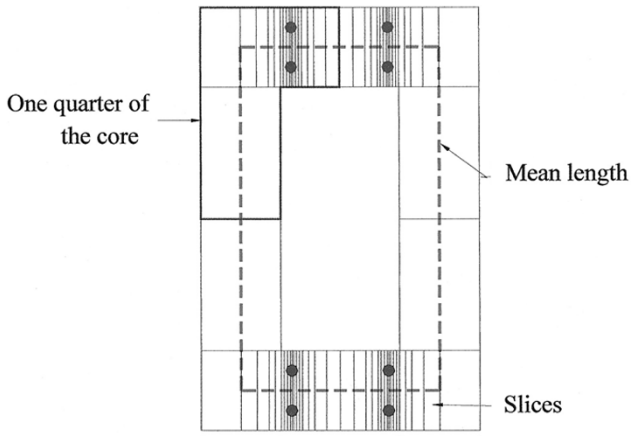

Fig. 6. Subdivision into n slices according to how H_{ta} varies.

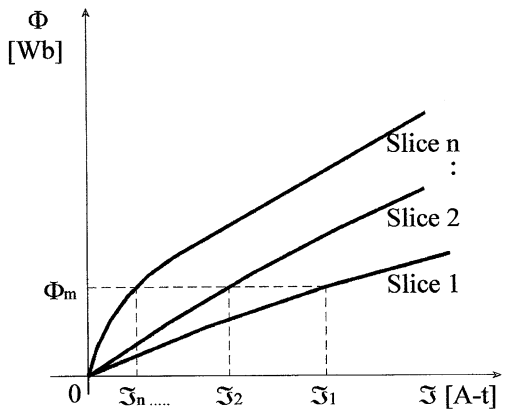

Fig. 7. Typical magnetization curves of the n core slices.

D. Equivalent Flux-mmf Curve of the Core

Step 4 is the calculation of the equivalent $\Phi - \Im$ curve of the core [4] by division of the core into n slices according to the variation of H_{ta} along the mean path length of the core. From the equivalent $\Phi - \Im$ curve the total mmf, $\Im$ is obtained. Due to symmetry, only one quarter of the core is considered (Fig. 6). In this example $n = 68$. Each slice has a specific value of H_{ta} and its own magnetization curve in terms of Φ and $\Im$ (Fig. 7).

The equivalent $\Phi - \Im$ curve is obtained from the sum of the mmf-s of each slice for the same value of $\Phi_{\rm m}$ [4]. The total

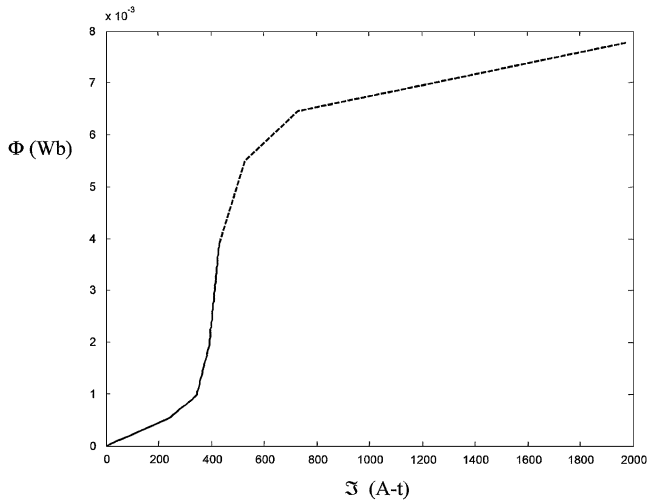

Fig. 8. Equivalent $\Phi - \Im$ curve corresponding to $I_a = \pm 10$ A.

mmf required to establish $\Phi_{\rm m}$ with local saturation is obtained from the equivalent $\Phi - \Im$ curve (Fig. 8). For a magnetic flux of $\Phi_{\rm m} = 5.359 \times 10^{-4}$ Wb with local saturation corresponding to $I_a = \pm 10$ A, the total mmf required is $\Im = 239.43$ A-t.

E. Core Reluctance With Local Saturation

Step 5 consists of obtaining the reluctance of the core *with* local saturation:

$$\Re = \frac{\Im}{\Phi_{\rm m}} = \frac{239.43}{5.359 \times 10^{-4}} \text{A-t}/Wb = 446781.12\ H^{-1}. \quad (3)$$

The increase in core reluctance is

$$\Delta\Re_{\rm m} = \Re - \Re_{\rm m} = 402127.26\ H^{-1}. \quad (4)$$

Finally, the equivalent length of the virtual air gap is obtained as

$$\ell_g = \Delta\Re_{\rm m}\mu_0 S = 2.5\ \text{mm} \quad (5)$$

where $S = (0.066\ \text{m}) \times (0.075\ \text{m}) = 0.00495\ \text{m}^2$ is the core cross-sectional area. For comparison, the computed and experimental values of ℓ_g given in [2] for the same level of saturation are 4.5 mm and 2.59 mm, respectively.

III. Results

The analytical method described in this paper was used to calculate the equivalent length of the virtual air gap. Fig. 9 shows a comparison between analytical [3] and experimental results [2]. In the analytical results, the calculation of the magnetic field is in one dimension (1-D). However, the magnetic field in the core used to obtain the experimental results, has a three-dimensional (3-D) distribution. Also, the analytical solution does not take into account core losses. Improvements to the method presented here are possible.

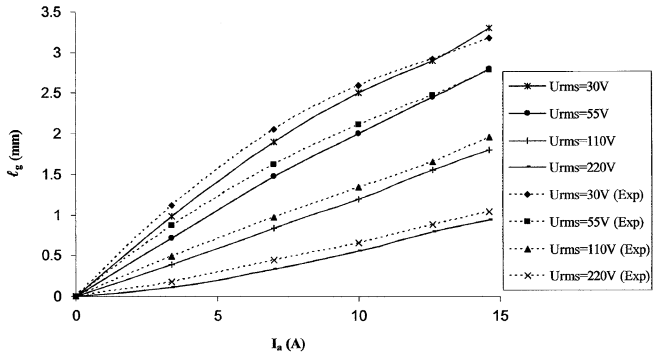

Fig. 9. Equivalent air gap length versus auxiliary winding current: comparison between experimental [2] and analytical [3] results for various rms supply voltages.

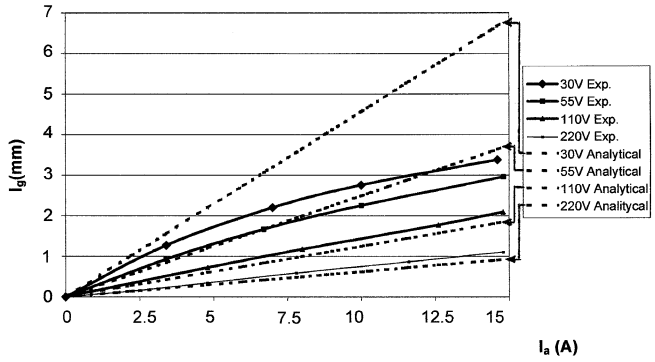

Fig. 10. Equivalent length of the virtual air gap. Comparison of experimental and analytical results in [2].

IV. Conclusion

Compared with experimental results, the above analytical approach gives a good approximation of the equivalent length of the virtual air gap as is evident from Fig. 9. This is especially true when the results are compared to the analytical results obtained in [2]; the latter are reproduced in Fig. 10 for comparison purposes.

The real advantage of the method presented here is that the distinct magnetic characteristics of each slice of the core is taken into consideration and, at the same time, the nonuniform magnetic flux distribution in saturated regions of the core is also accounted for.

References

[1] V. Molcrette, J. L. Kotny, J. P. Swan, and J. F. Brundy, "Reduction of inrush current in single-phase transformer using virtual air gap technique," *IEEE Trans. Magn.*, pt. I, vol. 34, no. 4, pp. 1192–1194, Jul. 1998.

[2] V. Rogez, D. Le Toriellec, V. Molcrette, J. L. Kotny, and J. F. Brudny, "Entrefer virtuel. Modélization des phénomènes," *Actes du Colloque Electrotechnique du Futur 2001*, pp. 367–372, Nov. 14–15, 2001. Thème 1-b, Paper no. P2–20 (in French).

[3] R. I. R. Barraza, "Virtual Air Gap Analysis," M.A.Sc. thesis, Univ. Toronto, Canada, 2003.

[4] A. Konrad, "Extension of the load line method to series magnetic circuits of nonuniform cross-section," in *Electromagnetic Fields in Electrical Engineering (ISEF'01)*, A. Krawczyk and S. Wiak, Eds. Amsterdam, The Netherlands: IOS Press, 2002, pp. 98–103.

Manuscript received February 7, 2005.